Letter

# Transverse instability and universal decay of spin spiral order in the Heisenberg model

Joaquin F. Rodriguez-Nieva [1], Alexander Schuckert [2,3] Dries Sels,[4,5] Michael Knap [2,3] and Eugene Demler[6]
[1] *Department of Physics, Stanford University, Stanford, California 94305, USA*
[2] *Department of Physics and Institute for Advanced Study, Technical University of Munich, 85748 Garching, Germany*
[3] *Munich Center for Quantum Science and Technology (MCQST), Schellingstrasse 4, D-80799 München, Germany*
[4] *Department of Physics, New York University, New York, 10003 New York, USA*
[5] *Center for Computational Quantum Physics, Flatiron Institute, New York, 10010 New York, USA*
[6] *Institute for Theoretical Physics, Wolfgang-Pauli-Str. 27, ETH Zurich, 8093 Zurich, Switzerland*

(Received 3 January 2021; revised 10 November 2021; accepted 20 January 2022; published 22 February 2022)

We analyze the intrinsic stability of spin spiral states in the two-dimensional Heisenberg model isolated from its environment. Our analysis reveals that the SU(2) symmetric point hosts a dynamic instability that is enabled by the existence of energetically favorable transverse deformations—both in real and spin space—of the spiral order. The instability is universal in the sense that it applies to systems with any spin number, spiral wave vector, and spiral amplitude. Unlike the Landau or modulational instabilities which require impurities or periodic potential modulation of an optical lattice, quantum fluctuations alone are sufficient to trigger the transverse instability. We analytically find the most unstable mode and its growth rate, and compare our analysis with phase-space methods. By adding an easy-plane exchange coupling that reduces the Hamiltonian symmetry from SU(2) to U(1), the stability boundary is shown to continuously interpolate between the modulational instability and the transverse instability. This suggests that the transverse instability is an intrinsic mechanism that hinders long-range phase coherence even in the presence of exchange anisotropy.

DOI: 10.1103/PhysRevB.105.L060302

Characterizing the mechanisms responsible for the breakdown of phase coherence in quantum systems is a fundamental problem with broad implications in quantum science and technology. The interplay between kinetic effects, interactions, and disorder gives rise to a wide range of phase relaxation mechanisms. In the simplest scenario, the phase coherence in a superfluid is subject to the Landau criterion [1], which defines an upper limit for the superfluid velocity: when the superfluid moves faster than the sound velocity, a spatially localized defect can trigger a superfluid instability that globally destroys phase coherence [2]. In the case of a Bose-Einstein condensate (BEC) in an optical lattice with spacing $a$, the characteristic lattice modulation $q_l = \pi/2a$ sets another limit for the superfluid wave vector above which a modulational instability occurs [3,4]. Such instability can be enhanced in the presence of strong interactions [5,6]. Rich physics and diverse mechanisms that destroy—and sometimes stabilize—the phase coherence have been discussed in the context of counterflowing superfluids [7], multicomponent [8] and spinor BECs [9–11], and superconductors [12–15], in the presence of extended disorder [16–19], dipolar interactions [20–22], and driving [23–27].

In this Letter, we inquire about the fate of spin spiral states [see Fig. 1(a)] in the isolated two-dimensional Heisenberg model. Such states can be created, for example, by globally rotating the spins around the $x$ axis by an angle $\theta$ and then using a magnetic field gradient with wave vector $\boldsymbol{q}$ to rotate the spins around the $z$ axis. Understanding the stability of spin spirals and the dynamics of decay under their own internal degrees of freedom is of relevance in many important scenarios. The nonequilibrium dynamics of spin spirals has recently been in the spotlight of several cold-atom experiments [28–30]. By tuning $\boldsymbol{q}$ and $\theta$, we can tune the energy and magnetization of the system and trigger interesting far-from-equilibrium phenomena, such as quantum turbulence [31,32], prethermalization [33], universal self-similar relaxation [34,35], and anomalous transport [36]. In addition,

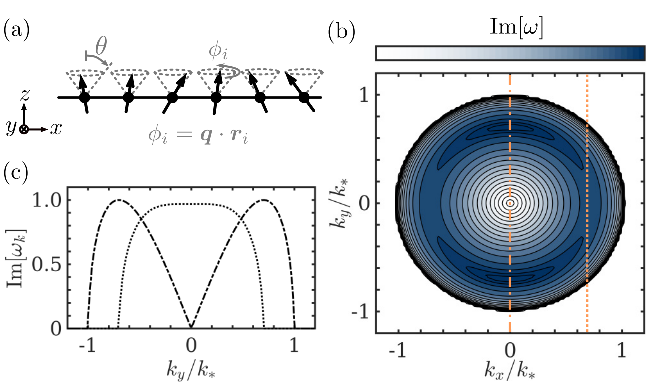


FIG. 1. (a) Schematics of a spin spiral parametrized by a wave vector $\boldsymbol{q}$ and angular amplitude $\theta$. (b) Imaginary part of the frequency of Bogoliubov modes. The wave vectors $k_{x,y}$ are relative to $\boldsymbol{q}$, which is assumed to be pointing in the $x$ direction ($k_* = q\sin\theta$). The fastest growing modes are transverse to $\boldsymbol{q}$, with $k_y \approx k_*/\sqrt{2}$. (c) Slice of (b) plotted at the line cuts $k_x/k_* = 0$ (dot-dashed line) and $k_x/k_* = 0.75$ (dotted line) and normalized with $1/\tau_*$ in Eq. (1). Parameters used: $\theta = \pi/4$, $q_x a = 0.5$, $q_y = 0$.

 

the stability of spin superfluids in ferromagnetic materials, promising for dissipationless spintronic applications [37–42], hinges on the stability of long-range coherence of a spin spiral. As such, our results are useful to understand the relevant modes that lead to spin superfluid decay when the coupling to a thermal bath is not important.

Our analysis reveals that the SU(2) symmetry of the Hamiltonian gives rise to a dynamic instability with different characteristics from previously studied instabilities. In particular, the instability (i) is enabled by gapless symmetry-allowed deformations of the order parameter rather than kinematic effects, (ii) is triggered by quantum fluctuations without the need for defects, disorder, or a lattice, and (iii) is universal in the sense that it affects systems with arbitrary spin number $S$, spiral wave vector, and spiral amplitude. The main physics can be understood by noticing that the SU(2) symmetry relaxes the topological constraint that protects the U(1) phase in superfluids [37]: while in usual superfluids the thermally activated creation of vortex-antivortex pairs or large kinematic fluctuations destroy coherence, the SU(2) symmetry alone furnishes additional "directions" (or rotation generators) in which the phase coherence can be destroyed for arbitrary values of $q$ (i.e., the critical wave vector is zero). As indicated in Fig. 1(b), the instability evolves by unwinding the spiral via growth of modes in a ring around the wave vector $\boldsymbol{q}$. Assuming $\boldsymbol{q} = (q_x, 0)$, the fastest growing mode has transverse wave vector $k_\perp \approx k_*/\sqrt{2}$ and grows with a rate $1/\tau_*$, with

$$k_* = |\boldsymbol{q}|\sin\theta, \quad \frac{1}{\tau_*} = JS\sin^2\theta[1-\cos(q_x a)], \tag{1}$$

until it becomes macroscopically occupied ($J$ is the exchange coupling). In addition, numerical simulations show that the constraint $\hat{S}_j^2 = S(S+1)$ of each spin regulates the instability growth, which peaks in a time $t \approx 4\tau_*$ (largely independent of $\boldsymbol{q}$, $\theta$, and $S$).

We analytically discuss dynamics in the SU(2) symmetric Heisenberg model for large $S$, but our conclusions are far more general. In particular, below we numerically show that the imprint of the ring of unstable modes survives even in the $S = 1/2$ limit for sufficiently small wave vectors. In addition, we show that the effect of the instability pervades away from the SU(2) symmetric point. Indeed, although it is known that the easy-plane *XXZ* model can host a stable superfluid state [39], we still observe a strong reduction of the critical wave vector for modulation instabilities (i.e., $|\boldsymbol{q}_c| = \pi/2a$) for a wide range of values of the exchange anisotropy. As such, manifestations of the transverse instability still exist in the presence of exchange anisotropy.

*Microscopic model*. We consider the two-dimensional Heisenberg model on a square lattice with exchange anisotropy,

$$\hat{H} = -\sum_{\langle j,j'\rangle} J\big(\hat{S}_j^x\hat{S}_{j'}^x + \hat{S}_j^y\hat{S}_{j'}^y\big) + J_z\hat{S}_j^z\hat{S}_{j'}^z, \tag{2}$$

where $\langle j, j'\rangle$ denotes summation over nearest neighbors. Each site contains a spin $S$ degree of freedom and periodic boundary conditions are assumed in each spatial direction. Our analysis is not affected by a Zeeman field, which is present in many relevant experiments: although a Zeeman field breaks the SU(2) symmetry of the Hamiltonian, its effect on dynamics can be removed by using a rotating frame. The initial condition is a spin spiral,

$$\langle\hat{S}_j^\pm\rangle = S\sin\theta e^{\pm i\boldsymbol{q}\cdot\boldsymbol{r}_j}, \quad \langle\hat{S}_j^z\rangle = S\cos\theta, \tag{3}$$

with $\hat{S}_j^\pm = \hat{S}_j^x \pm i\hat{S}_j^y$.

*Bogoliubov analysis*. The equations of motion of the spin operators are given by $\partial_t\hat{\boldsymbol{S}}_j = J\sum_{j'\in\mathcal{N}_j}\hat{\boldsymbol{S}}_j \times (\hat{\boldsymbol{S}}_{j'} + \epsilon\hat{S}_{j'}^z\boldsymbol{z})$, with $\epsilon = (J_z - J)/J$, $\mathcal{N}_j$ the nearest neighbors of site $j$, and $\boldsymbol{z}$ a unit vector. We first analyze the linearized dynamics at short times using the approximation $\langle\hat{S}_j^\alpha\hat{S}_{j'}^\beta\rangle \approx \langle\hat{S}_j^\alpha\rangle\langle\hat{S}_{j'}^\beta\rangle$, which gives rise to the equations of motion

$$\dot{S}_j^\pm = \mp iJ\sum_{j'\in\mathcal{N}_j}\big[(1+\epsilon)S_j^\pm S_{j'}^z - S_{j'}^\pm S_j^z\big],$$
$$\dot{S}_j^z = \frac{iJ}{2}\sum_{j'\in\mathcal{N}_j}\big[S_j^+S_{j'}^- - S_j^-S_{j'}^+\big], \tag{4}$$

with $\langle\hat{S}_j^\alpha\rangle = S_j^\alpha$. Hereafter, energy and inverse time are expressed in units of $JS$ and wave vectors in units of $1/a$. Using the initial conditions in Eq. (3), it can be shown that the solution $\bar{S}_j^\pm(t) = S\sin\theta e^{\pm i(\boldsymbol{q}\cdot\boldsymbol{r}_j+\mu t)}$, $\bar{S}_j^z = S\cos\theta$, is a steady-state solution of Eq. (4) with oscillation frequency $\mu = 2\cos\theta[(1+\epsilon)2 - \cos q_x - \cos q_y]$. Therefore, one can systematically incorporate the effects of quantum fluctuations on top of this classical stationary solution through a Bogoliubov analysis, as we discuss next.

We proceed to analyze the stability of the spiral in the isotropic exchange case, $\epsilon = 0$. We parametrize fluctuations on top of the steady-state solution using the $xy$ components of magnetization, $S_j^\pm = \bar{S}_j^\pm + \delta S_j^\pm$; this implies that our parametrization is singular at $\theta = \pi/2$, but taking the limit $\theta \to \pi/2$ at the end still yields the correct result (a parametrization in polar coordinates that is nonsingular at $\theta = \pi/2$, but more cumbersome, is discussed in the Supplemental Material [43]). Going into momentum space and expressing modes relative to the wave vector and frequency of the spiral, $\delta S_j^\pm = e^{\pm i(\boldsymbol{q}\cdot\boldsymbol{r}_j+\mu t)}\sum_{\boldsymbol{k}} e^{i(\boldsymbol{k}\cdot\boldsymbol{r}_j+\omega_{\boldsymbol{k}}t)}\delta S_{\boldsymbol{k}\pm\boldsymbol{q}}^\pm$, the linearized equations of motion are (see Supplemental Material [43])

$$\begin{pmatrix}\omega_{\boldsymbol{k}} + \varepsilon_{\boldsymbol{q}+\boldsymbol{k}} + \frac{\Delta_{\boldsymbol{k}}}{2} - \mu & \frac{\Delta_{\boldsymbol{k}}}{2}\\ -\frac{\Delta_{\boldsymbol{k}}}{2} & \omega_{\boldsymbol{k}} - \varepsilon_{\boldsymbol{q}-\boldsymbol{k}} - \frac{\Delta_{\boldsymbol{k}}}{2} + \mu\end{pmatrix}\delta\boldsymbol{S} = 0. \tag{5}$$

Here, $\delta\boldsymbol{S} = (\delta S_{\boldsymbol{q}+\boldsymbol{k}}^+, \delta S_{\boldsymbol{k}-\boldsymbol{q}}^-)^{\mathrm{t}}$, and $\varepsilon_{\boldsymbol{p}}$, $\Delta_{\boldsymbol{k}}$ are

$$\varepsilon_{\boldsymbol{q}\pm\boldsymbol{k}} = \cos\theta(\gamma_0 - \gamma_{\boldsymbol{q}\pm\boldsymbol{k}}), \quad \Delta_{\boldsymbol{k}} = \sin\theta\tan\theta(\gamma_{\boldsymbol{q}} - \gamma_{\boldsymbol{k}}), \tag{6}$$

where we defined $\gamma_{\boldsymbol{k}} = 2(\cos k_x + \cos k_y)$. Note that the Bogoliubov analysis can be generalized to next-nearest-neighbor interactions by modifying the definition of $\gamma_{\boldsymbol{k}}$ accordingly. From Eq. (6), we note that the value of $\mu$ is $\mu = \varepsilon_{\boldsymbol{q}}$. The frequencies of the Bogoliubov modes are

$$\omega_{\boldsymbol{k}} = \frac{\varepsilon_{\boldsymbol{q}+\boldsymbol{k}} - \varepsilon_{\boldsymbol{q}-\boldsymbol{k}}}{2} \pm \frac{1}{2}\sqrt{\Delta\varepsilon(\Delta\varepsilon + 2\Delta_{\boldsymbol{k}})}, \tag{7}$$

where $\Delta\varepsilon = \varepsilon_{\boldsymbol{q}+\boldsymbol{k}} + \varepsilon_{\boldsymbol{q}-\boldsymbol{k}} - 2\varepsilon_{\boldsymbol{q}}$ can be interpreted as the kinetic energy cost of unbinding two quasiparticles from the macroscopically occupied mode $\boldsymbol{q}$. For large spiral wave vectors, $q_x, q_y > \pi/2$, $\Delta\varepsilon$ can be negative because of the negative mass of bare particles and gives rise to the previously studied modulational instability [3]. For $q_x, q_y < \pi/2$, however, $\Delta\varepsilon$ is strictly positive and the condition for the mode $S^+_{\boldsymbol{q}+\boldsymbol{k}}$ to be unstable (i.e., $\omega''_{\boldsymbol{k}} = \mathrm{Im}[\omega_{\boldsymbol{k}}] \neq 0$) is given by

$$\varepsilon_{\boldsymbol{q}+\boldsymbol{k}} + \varepsilon_{\boldsymbol{q}-\boldsymbol{k}} - 2\varepsilon_{\boldsymbol{q}} + 2\Delta_{\boldsymbol{k}} < 0. \tag{8}$$

It is instructive to analyze the condition (8) in the limit of small $\boldsymbol{q}$ and $\theta$ such that we can contrast it with the Landau instability. The initial spin spiral state can be interpreted as a macroscopically occupied state (i.e., a quasicondensate) with wave vector $q$ on top of the ferromagnetic ground state. Upon approaching the classical limit ($S \to \infty$), the magnon interaction vanishes as $1/S$. As a result, the spiral does not decay in the classical limit. At the isotropic point and for finite $S$, Eq. (8) reflects an energy balance condition resulting from unbinding two magnons of energy $\varepsilon_{\boldsymbol{q}\pm\boldsymbol{k}} \approx JSa^2(\boldsymbol{q} \pm \boldsymbol{k})^2$ and with a *momentum-dependent* pairing energy $\Delta_{\boldsymbol{k}} \approx -JSa^2 \sin^2\theta(\boldsymbol{q}^2 - \boldsymbol{k}^2)$. Importantly, $\Delta_{\boldsymbol{k}}$ is attractive in a ring of radius $|\boldsymbol{k}| \lesssim |\boldsymbol{q}|$. Attractive magnon-magnon interactions are known to give rise to magnon bound states in one dimension (1D) [44] and its momentum dependence has been shown to result in unusual quasiparticle relaxation [45] and hydrodynamic behavior [46,47]. Equation (8) dictates that independently of $S$, the growth of modes with small wave vectors $\boldsymbol{k}$ relative to $\boldsymbol{q}$ is energetically favorable (a large value of $\boldsymbol{k}$, on the other hand, is penalized by a large kinetic energy cost, $\varepsilon_{\boldsymbol{q}+\boldsymbol{k}} + \varepsilon_{\boldsymbol{q}-\boldsymbol{k}} - 2\varepsilon_{\boldsymbol{q}} \propto \boldsymbol{k}^2$). In contrast, usual superfluids have a *repulsive* hard-core interaction $\Delta_{\boldsymbol{k}} = gn > 0$ that is momentum independent, which means that the kinetic energy of the superfluid has to be sufficiently large (i.e., there is a finite critical wave vector) for the instability criterion (8) to be satisfied ($g$: local interaction; $n$: density).

More generally, Eq. (8) gives rise to unstable modes for any value of $\boldsymbol{q}$ and $\theta$. To analytically find the most unstable mode when $\boldsymbol{q} = (q_x, 0)$, we maximize $\omega''_{\boldsymbol{k}}$ under the constraint $k_x = 0$ [note that the fastest growing mode in Fig. 1(a) is transverse to $\boldsymbol{q}$]. In this case, we obtain

$$\omega''_{\boldsymbol{k}} = 2\sqrt{(1-\cos k_y)\big[(1-\cos k_y) - \sin^2\theta(1-\cos q_x)\big]}. \tag{9}$$

From this, we see that the maximum of $\omega''_{\boldsymbol{k}}$ occurs at $k_y = \tilde{k}_y$, with $\tilde{k}_y$ satisfying $1 - \cos\tilde{k}_y = \sin^2\theta(1-\cos q_x)/2$, and such mode grows with a rate $\max(\omega''_{\boldsymbol{k}}) = \frac{1}{\tau_*}$ in Eq. (1). Equation (9) also defines the volume in phase space of unstable modes, which is bounded by the wave vector $k_*$ satisfying the condition $1 - \cos k_* = \sin^2\theta[1 - \cos q_x]$. In the limit of small $q_x$, we obtain $\tilde{k}_y \approx k_*/\sqrt{2}$, with $k_*$ defined in Eq. (1).

*Phase-space methods.* To complement the Bogoliubov analysis, we compute real-time dynamics of the spiral decay by incorporating quantum fluctuations using the truncated Wigner approximation (TWA) [48]. Defining $\langle\hat{\boldsymbol{S}}^\perp_j\rangle$ as the transverse magnetization of the initial condition (3), we assume Gaussian fluctuations of $\hat{\boldsymbol{S}}^\perp_j$ given by $\langle\hat{\boldsymbol{S}}^\perp_j\rangle = 0$ and $\langle\hat{\boldsymbol{S}}^\perp_j \cdot \hat{\boldsymbol{S}}^\perp_j\rangle = S$.

Figure 2(a) shows a single realization of the TWA noise for a spin spiral with parameters $\theta = \pi/4$ and $q_x = 0.5$ (same parameters as in Fig. 1). Independently of the spin number $S$, we consistently observe growth of unstable modes that lead to a disordered state. Analysis of the connected correlation $\langle\hat{S}^x_{-\boldsymbol{K}}\hat{S}^x_{\boldsymbol{K}}\rangle_c = \langle\hat{S}^x_{-\boldsymbol{K}}\hat{S}^x_{\boldsymbol{K}}\rangle - \langle\hat{S}^x_{-\boldsymbol{K}}\rangle\langle\hat{S}^x_{\boldsymbol{K}}\rangle$ [shown in Fig. 2(b), with $\boldsymbol{K}$ the absolute wave vector] reveals that the spiral state is primarily decaying into modes located in a ring around the wave vector $\boldsymbol{q}$, preferentially in the direction perpendicular to $\boldsymbol{q}$, thus confirming the Bogoliubov analysis above.

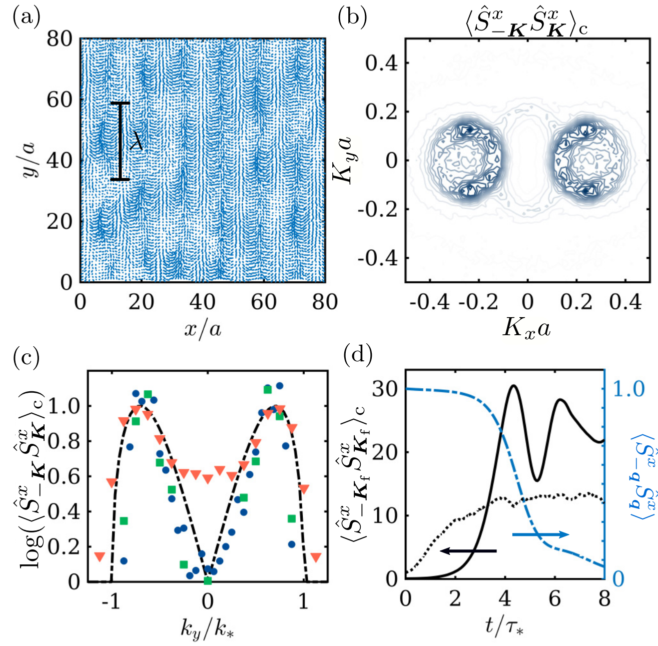


FIG. 2. (a) Real-space snapshot of a single TWA realization at $t/\tau_* = 3.5$; see Eq. (1). Shown are snapshots of the spins $\hat{\boldsymbol{S}}_j$ projected on the $xy$ plane. Indicated with a bar is the wavelength in the $y$ direction of the fastest growing mode. (b) Contour plot showing the connected correlation $\langle\hat{S}^x_{-\boldsymbol{K}}\hat{S}^x_{\boldsymbol{K}}\rangle_c$ corresponding to (a). Consistent with the Bogoliubov analysis, the plot exhibits a ring of unstable modes around $\boldsymbol{q}$ with size $k_* \approx q_x \sin\theta$ and a maximal amplitude transverse to $\boldsymbol{q}$. Parameters used in (a) and (b): $\theta = \pi/4$, $q_x = 0.25$, $q_y = 0$, $S = 10$ averaged over 50 realizations. (c) Spatial-temporal scaling of $\langle\hat{S}^x_{-\boldsymbol{K}}\hat{S}^x_{\boldsymbol{K}}\rangle_c$. Shown is the logarithm of $\langle\hat{S}^x_{-\boldsymbol{K}}\hat{S}^x_{\boldsymbol{K}}\rangle_c$ for $\boldsymbol{K} = (q_x, k_y)$ and $t/\tau_* = 3.5$, and for different initial conditions: $(q_x, \theta) = (0.25, \pi/2)$ (circles), $(0.5, \pi/2)$ (squares), and $(0.25, \pi/4)$ (triangles) and $S = 10$. The dot-dashed line is the Bogoliubov $\mathrm{Im}[\omega]$ in Eq. (9) as a guide to the eye. (d) Growth of the most unstable mode, $\boldsymbol{K}_f = (q_x, \tilde{k}_y)$, showing saturation and subsequent oscillations for $S = 10$ (solid line) and $S = 1/2$ (dotted lines). Also shown is the depletion of the spin spiral (dash-dotted line).

In addition, Fig. 2(c) shows the scaling of fluctuations for wave vectors $\boldsymbol{K} = (q_x, k_y)$ and various initial conditions at the rescaled time $t/\tau_* = 3.5$. Given that we expect unstable modes to grow as $S^+_{\boldsymbol{K}}(t) \approx S^+_{\boldsymbol{K}}(0)e^{t/\tau_K}$, the $y$ axis is plotted in logarithmic scale and the correlation $\langle\hat{S}^x_{-\boldsymbol{K}}\hat{S}^x_{\boldsymbol{K}}\rangle_c$ is normalized with the maximum value as a function of $k_y$ for each initial condition. We observe excellent agreement with the Bogoliubov analysis for all $\boldsymbol{q}$ and $\theta$.

*Instability growth and self-regularization.* Going beyond the linear stability analysis, we inquire about the intermediate timescale dynamics of instability growth. Figure 2(d) shows the decay of the spin spiral and multiple stages in the evolution of the most unstable mode: (i) initial growth compatible

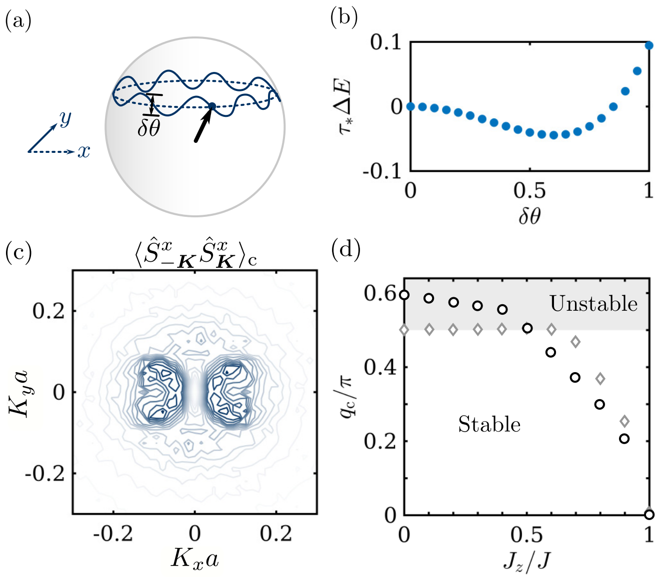


FIG. 3. (a) Schematics of the most favorable deformation of the spin spiral order and (b) the corresponding energy shift with respect to the spiral state. Shown in (a) is the trajectory of the magnetization vector by moving on the lattice in the $x$ (dotted line) and $y$ (solid line) directions, and $\delta\theta$ is the amplitude of deformation; see definition in main text. (c) Contour plot showing the connected component of $\langle \hat{S}^x_{-\boldsymbol{K}}\hat{S}^x_{\boldsymbol{K}}\rangle$ for $S = 1/2$, $q_x a = 0.12$, and $\theta = \pi/2$. (d) Stability boundary showing the critical momentum $q_c$ as a function of exchange anisotropy for a spiral amplitude of $\theta = \pi/4$ (black circles), $\theta = 0.1$ (gray diamonds), and $S \to \infty$. The shaded area indicates the parameter space region of the modulational instability.

with the Bogoliubov analysis above, (ii) saturation, and (iii) coherent oscillations prior to equilibration. Unlike the usual instabilities in BEC where unstable modes grow exponentially for long times, the local constraint $\hat{S}_j^2 = S(S+1)$ and the conservation of total magnetization regulate the growth of the transverse spin modulation at relatively short times, analogously to Refs. [33,49,50]. We observe that saturation occurs at $t \approx 4\tau_*$, irrespective of the value of $S$, $\boldsymbol{q}$, and $\theta$ (see the Supplemental Material [43]).

The existence of unstable modes in the linearized analysis and the small oscillations in Fig. 2(d) are linked to the existence of smooth, symmetry-allowed deformations of the spin spiral order with a valley-shaped potential. Using the insights gained from the Bogoliubov analysis, we propose a simple ansatz for a transverse spin texture given by $S_j^{\pm} = S\sin\theta_i e^{\pm i\boldsymbol{q}\cdot\boldsymbol{r}_j}$ and $S_j^z = S\cos\theta_j$, with $\theta_j = \bar{\theta} + 2\delta\theta\cos(\tilde{k}_y y_i)$ and $\tilde{k}_y$ defined below Eq. (9) [see Fig. 3(a)]. The value of $\delta\theta$ controls the amplitude of transverse spin deformations around $\bar{\theta}$ and is modulated by the transverse wave vector $\tilde{k}_y$. This ansatz trivially satisfies $\sum_j S_j^{\pm} = 0$ for all values of $\bar{\theta}$ and $\delta\theta$, and the condition $\frac{1}{N}\sum_j S_j^z = S\cos\theta$ defines a constraint that links $\bar{\theta}$ and $\delta\theta$. Because we recover Eq. (3) when $\bar{\theta} = \theta$ and $\delta\theta = 0$, our ansatz is smoothly connected to the original spiral and preserves its total magnetization. Figure 3(b) shows that increasing the transverse modulation $\delta\theta$ reduces the energy of the spin spiral. In addition, the observed oscillations in Fig. 2(d) can be interpreted as amplitude oscillations on a valley-shaped potential. The same argument can be applied to any value of $\boldsymbol{k}$ that satisfies the instability condition (8), but the valley is deepest for $\boldsymbol{K} = (q_x, \tilde{k}_y)$.

*Crossover to the quantum regime*. The stability analysis above relies on a $1/S$ expansion of the equations of motion, opening the question on its validity in the experimentally relevant $S = 1/2$ case. The competition between quantumness in the $S \to 1/2$ limit and classicality in the $\boldsymbol{q} \to 0$ limit suggests that a smeared, but still observable, ring of unstable modes is obtained for finite but small $\boldsymbol{q}$ and $S = 1/2$. Indeed, our numerics reveal that strong quantum fluctuations suppress the exponential growth of unstable modes and smear out coherent oscillations in the two-point correlation function [see Fig. 2(d)], but the latter still exhibits an imprint of the ring of unstable modes [see Fig. 3(c)]. Remarkably, we also find that our stability analysis is valid in the one-dimensional Heisenberg model despite integrability and reduced dimensionality, as shown with matrix product states and TWA in the Supplemental Material [43] (in this case, the most unstable modes are necessarily collinear with $q_x$).

*Crossover to modulational instability*. To study the crossover between the transverse instability in the Heisenberg model ($J_z = J$) to the modulational instability that characterizes a superfluid on a lattice, we extend the Bogoliubov analysis for values of $J_z < J$ (see details in the Supplemental Material [43]). Tuning $J_z$ can be realized experimentally using Feshbach resonances, dipolar interactions, or lattice shacking [51–55]. The anisotropic exchange energetically penalizes the transverse deformation of the spin spiral order. In the language of the stability condition in Eq. (8), the pairing $\Delta_{\boldsymbol{k}}$ becomes repulsive, $\Delta_{\boldsymbol{k}} \approx (J - J_z)$, and $\varepsilon_{\boldsymbol{k}}$ becomes linearly dispersing. Although reducing the SU(2) symmetry to U(1) has a stabilizing effect on the spin spiral state, there is still a strong reduction of the critical wave vector close to the SU(2) symmetric point, as shown in Fig. 3(d). This suggests that the instability mechanism that we describe is also relevant for systems with weak anisotropic exchange.

*Conclusions*. We analyzed a class of dynamic instability which is enabled by the topology of the order parameter manifold rather than kinematic effects. Such instability is an intrinsic mechanism that hinders long-range phase coherence in spin systems. While the mechanism that we discuss is intrinsic to the Heisenberg model with ferromagnetic ordering, open problems include understanding the enhancement of the instability in the presence of disorder and long-range interactions, and understanding the mechanisms of decay in systems with antiferromagnetic ordering and different lattice types. In addition, extending our simulations to longer timescales in order to obtain a holistic perspective of thermalization, which captures the growth of unstable modes and subsequent quasiparticle relaxation, remains an important challenge.

*Acknowledgments.*. We thank Marin Bukov, Wen Wei Ho, Asier Piñeiro Orioli, Daniel Podolsky, Ana Maria Rey, Amir Yacoby, Tony Zhou and Bihui Zhu for valuable insights and discussions. J.F.R-N. acknowledges the Gordon and Betty Moore Foundation's EPiQS Initiative through Grants No. GBMF4302 and No. GBMF8686, the 2019 KITP program *Spin and Heat Transport in Quantum and Topological Materials*, and the National Science Foundation under Grant No.

NSF PHY-1748958. A.S. and M.K. acknowledge support from the Technical University of Munich, Institute for Advanced Study, funded by the German Excellence Initiative and the European Union FP7 under Grant Agreement No. 291763, the Max Planck Gesellschaft (MPG) through the International Max Planck Research School for Quantum Science and Technology (IMPRS-QST), the Deutsche Forschungsgemeinschaft (DFG, German Research Foundation) under Germany's Excellence Strategy-EXC-2111-390814868, DFG TRR80, and DFG Grant No. KN1254/1-2, and from the European Research Council (ERC) under the European Union's Horizon 2020 research and innovation programme (Grant Agreement No. 851161). E.D. acknowledges support from the Harvard-MIT CUA, AFOSR-MURI: Photonic Quantum Matter (Award No. FA95501610323), and the DARPA DRINQS program (Award No. D18AC00014).

[1] L. Landau, Theory of the superfluidity of Helium II, Phys. Rev. **60**, 356 (1941).
[2] Z. Dutton, M. Budde, C. Slowe, and L. V. Hau, Observation of quantum shock waves created with ultra-compressed slow light pulses in a Bose-Einstein condensate, Science **293**, 663 (2001).
[3] B. Wu and Q. Niu, Landau and dynamical instabilities of the superflow of Bose-Einstein condensates in optical lattices, Phys. Rev. A **64**, 061603(R) (2001).
[4] L. Fallani, L. De Sarlo, J. E. Lye, M. Modugno, R. Saers, C. Fort, and M. Inguscio, Observation of dynamical instability for a Bose-Einstein Condensate in a Moving 1D Optical Lattice, Phys. Rev. Lett. **93**, 140406 (2004).
[5] A. Polkovnikov, E. Altman, E. Demler, B. Halperin, and M. D. Lukin, Decay of superfluid currents in a moving system of strongly interacting bosons, Phys. Rev. A **71**, 063613 (2005).
[6] E. Altman, A. Polkovnikov, E. Demler, B. I. Halperin, and M. D. Lukin, Superfluid-Insulator Transition in a Moving System of Interacting Bosons, Phys. Rev. Lett. **95**, 020402 (2005).
[7] A. A. Norrie, R. J. Ballagh, and C. W. Gardiner, Quantum turbulence in condensate Collisions an Application of the Classical Field Method, Phys. Rev. Lett. **94**, 040401 (2005).
[8] H. Takeuchi, S. Ishino, and M. Tsubota, Binary Quantum Turbulence Arising from Countersuperflow Instability in Two-Component Bose-Einstein Condensates, Phys. Rev. Lett. **105**, 205301 (2010).
[9] R. W. Cherng, V. Gritsev, D. M. Stamper-Kurn, and E. Demler, Dynamical Instability of the XY Spiral State of Ferromagnetic Condensates, Phys. Rev. Lett. **100**, 180404 (2008).
[10] R. W. Cherng and E. Demler, Magnetoroton Softening in Rb Spinor Condensates With Dipolar Interactions, Phys. Rev. Lett. **103**, 185301 (2009).
[11] K. Fujimoto and M. Tsubota, Counterflow instability and turbulence in a spin-1 spinor Bose-Einstein condensate, Phys. Rev. A **85**, 033642 (2012).
[12] J. S. Langer and V. Ambegaokar, Intrinsic resistive transition in narrow superconducting channels, Phys. Rev. **164**, 498 (1967).
[13] D. E. McCumber and B. I. Halperin, Time scale of intrinsic resistive fluctuations in thin superconducting wires, Phys. Rev. B **1**, 1054 (1970).
[14] D. E. Sheehy and P. M. Goldbart, Intrinsic resistivity and the SO(5) theory of high-temperature superconductors, Phys. Rev. B **57**, R8131 (1998).
[15] B. I. Halperin, G. Refael, and E. Demler, Resistance in superconductors, Intl. J. Mod. Phys. B **24**, 4039 (2010).
[16] T. Paul, P. Schlagheck, P. Leboeuf, and N. Pavloff, Superfluidity Versus Anderson Localization in a Dilute Bose Gas, Phys. Rev. Lett. **98**, 210602 (2007).
[17] M. Albert, T. Paul, N. Pavloff, and P. Leboeuf, Dipole Oscillations of a Bose-Einstein Condensate in the Presence of Defects and Disorder, Phys. Rev. Lett. **100**, 250405 (2008).
[18] M. Albert, T. Paul, N. Pavloff, and P. Leboeuf, Breakdown of the superfluidity of a matter wave in a random environment, Phys. Rev. A **82**, 011602(R) (2010).
[19] T. Haga and M. Ueda, Anomalous phase fluctuations of a superfluid flowing in a random potential, Phys. Rev. Res. **2**, 043316 (2020).
[20] L. Santos, G. V. Shlyapnikov, P. Zoller, and M. Lewenstein, Bose-Einstein Condensation in Trapped Dipolar Gases, Phys. Rev. Lett. **85**, 1791 (2000).
[21] K. Góral and L. Santos, Ground state and elementary excitations of single and binary Bose-Einstein condensates of trapped dipolar gases, Phys. Rev. A **66**, 023613 (2002).
[22] L. Santos, G. V. Shlyapnikov, and M. Lewenstein, Roton-Maxon Spectrum and Stability of Trapped Dipolar Bose-Einstein Condensates, Phys. Rev. Lett. **90**, 250403 (2003).
[23] G. Bertotti, I. Mayergoyz, and C. Serpico, Spin-wave instabilities in Landau–Lifshitz–Gilbert dynamics, Phys. B: Condens. Matter **306**, 106 (2001).
[24] A. J. E. Kreil, D. A. Bozhko, H. Y. Musiienko-Shmarova, V. I. Vasyuchka, V. S. L'vov, A. Pomyalov, B. Hillebrands, and A. A. Serga, From kinetic instability to Bose-Einstein Condensation and Magnon Supercurrents, Phys. Rev. Lett. **121**, 077203 (2018).
[25] K. Wintersperger, M. Bukov, J. Näger, S. Lellouch, E. Demler, U. Schneider, I. Bloch, N. Goldman, and M. Aidelsburger, Parametric Instabilities of Interacting Bosons in Periodically-Driven 1D Optical Lattices, Phys. Rev. X **10**, 011030 (2020).
[26] M. Bukov, S. Gopalakrishnan, M. Knap, and E. Demler, Prethermal Floquet Steady States and Instabilities in the Periodically Driven, Weakly Interacting Bose-Hubbard Model, Phys. Rev. Lett. **115**, 205301 (2015).
[27] T. Boulier, J. Maslek, M. Bukov, C. Bracamontes, E. Magnan, S. Lellouch, E. Demler, N. Goldman, and J. V. Porto, Parametric Heating in a 2D Periodically Driven Bosonic System Beyond the Weakly Interacting Regime, Phys. Rev. X **9**, 011047 (2019).
[28] A. B. Bardon, S. Beattie, C. Luciuk, W. Cairncross, D. Fine, N. S. Cheng, G. J. A. Edge, E. Taylor, S. Zhang, S. Trotzky, and J. H. Thywissen, Transverse demagnetization dynamics of a unitary Fermi gas, Science **344**, 722 (2014).
[29] S. Hild, T. Fukuhara, P. Schauß, J. Zeiher, M. Knap, E. Demler, I. Bloch, and C. Gross, Far-from-Equilibrium Spin Transport in Heisenberg Quantum Magnets, Phys. Rev. Lett. **113**, 147205 (2014).
[30] R. C. Brown, R. Wyllie, S. B. Koller, E. A. Goldschmidt, M. Foss-Feig, and J. V. Porto, Two-dimensional superexchange-

mediated magnetization dynamics in an optical lattice, Science **348**, 540 (2015).
[31] M. Tsubota, Quantum turbulence from superfluid helium to atomic Bose-Einstein condensates, J. Phys.: Condens. Matter **21**, 164207 (2009).
[32] J. F. Rodriguez-Nieva, Turbulent relaxation after a quench in the Heisenberg model, Phys. Rev. B **104**, L060302 (2021).
[33] M. Babadi, E. Demler, and M. Knap, Far-from-Equilibrium Field Theory of Many-Body Quantum Spin Systems Prethermalization and Relaxation of Spin Spiral States in Three Dimensions, Phys. Rev. X **5**, 041005 (2015).
[34] A. Piñeiro Orioli, K. Boguslavski, and J. Berges, Universal self-similar dynamics of relativistic and nonrelativistic field theories near nonthermal fixed points, Phys. Rev. D **92**, 025041 (2015).
[35] J. Berges, Nonequilibrium quantum fields from cold atoms to cosmology, arXiv:1503.02907.
[36] N. Jepsen, J. Amato-Grill, I. Dimitrova, W. W. Ho, E. Demler, and W. Ketterle, Spin transport in a tunable Heisenberg model realized with ultracold atoms, Nature (London) **588**, 403 (2020).
[37] E. Sonin, Spin currents and spin superfluidity, Adv. Phys. **59**, 181 (2010).
[38] D. A. Bozhko, A. A. Serga, P. Clausen, V. I. Vasyuchka, F. Heussner, G. A. Melkov, A. Pomyalov, V. S. L'vov, and B. Hillebrands, Supercurrent in a room-temperature Bose-Einstein magnon condensate, Nat. Phys. **12**, 1057 (2016).
[39] S. Takei and Y. Tserkovnyak, Superfluid Spin Transport through Easy-Plane Ferromagnetic Insulators, Phys. Rev. Lett. **112**, 227201 (2014).
[40] K. Nakata, K. A. van Hoogdalem, P. Simon, and D. Loss, Josephson and persistent spin currents in Bose-Einstein condensates of magnons, Phys. Rev. B **90**, 144419 (2014).
[41] C. Sun, T. Nattermann, and V. L. Pokrovsky, Unconventional Superfluidity in Yttrium Iron Garnet Films, Phys. Rev. Lett. **116**, 257205 (2016).
[42] E. B. Sonin, Spin superfluidity and spin waves in YIG films, Phys. Rev. B **95**, 144432 (2017).
[43] See Supplemental Material at http://link.aps.org/supplemental/10.1103/PhysRevB.105.L060302 for (i) technical details about the derivation of the Bogoliubov analysis, (ii) complementary numerical results of the instability growth for various initial conditions, and (iii) comparison with MPS simulations in 1D. This includes [56].
[44] D. C. Mattis, *The Theory of Magnetism Made Simple* (World Scientific, Singapore, 2006).
[45] S. Bhattacharyya, J. F. Rodriguez-Nieva, and E. Demler, Universal Prethermal Dynamics in Heisenberg Ferromagnets, Phys. Rev. Lett. **125**, 230601 (2020).
[46] E. Iacocca, T. J. Silva, and M. A. Hoefer, Breaking of Galilean Invariance in the Hydrodynamic Formulation of Ferromagnetic Thin Films, Phys. Rev. Lett. **118**, 017203 (2017).
[47] J. F. Rodriguez-Nieva, D. Podolsky, and E. Demler, Hydrodynamic sound modes and Galilean symmetry breaking in a magnon fluid, arXiv:1810.12333.
[48] A. Polkovnikov, Phase space representation of quantum dynamics, Ann. Phys. **325**, 1790 (2010).
[49] J. Berges and J. Serreau, Parametric Resonance in Quantum Field Theory, Phys. Rev. Lett. **91**, 111601 (2003).
[50] J. Berges, A. Rothkopf, and J. Schmidt, Nonthermal Fixed Points Effective Weak Coupling for Strongly Correlated Systems far from Equilibrium, Phys. Rev. Lett. **101**, 041603 (2008).
[51] S. Trotzky, P. Cheinet, S. Fölling, M. Feld, U. Schnorrberger, A. M. Rey, A. Polkovnikov, E. A. Demler, M. D. Lukin, and I. Bloch, Time-resolved observation and control of superexchange interactions with ultracold atoms in optical lattices, Science **319**, 295 (2008).
[52] B. Yan, S. A. Moses, B. Gadway, J. P. Covey, K. R. A. Hazzard, A. M. Rey, D. S. Jin, and J. Ye, Observation of dipolar spin-exchange interactions with lattice-confined polar molecules, Nature (London) **501**, 521 (2013).
[53] C. V. Parker, L.-C. Ha, and C. Chin, Direct observation of effective ferromagnetic domains of cold atoms in a shaken optical lattice, Nat. Phys. **9**, 769 (2013).
[54] C.-L. Hung, A. González-Tudela, J. I. Cirac, and H. J. Kimble, Quantum spin dynamics with pairwise-tunable, long-range interactions, Proc. Natl. Acad. Sci. **113**, E4946 (2016).
[55] E. J. Davis, G. Bentsen, L. Homeier, T. Li, and M. H. Schleier-Smith, Photon-Mediated Spin-Exchange Dynamics of Spin-1 Atoms, Phys. Rev. Lett. **122**, 010405 (2019).
[56] J. Hauschild and F. Pollman, Efficient numerical simulations with Tensor Networks Tensor Network Python (TeNPy), SciPost Phys. Lect. **5** (2018).